Multibody Syst Dyn (2009) 21: 213–231
DOI 10.1007/s11044-008-9136-0

Vertical dynamics of the Maglev vehicle Transrapid

Nora Hägele · Florian Dignath

Received: 17 May 2008 / Accepted: 23 October 2008 / Published online: 22 November 2008

Abstract The Maglev vehicle Transrapid is levitated by magnetic forces which pull the vehicles levitation frames toward the guideway from below. The magnets possess poles with alternating fluxes which are part of the synchronous long stator linear motor. Although the Transrapid glides along its guideway without mechanical contact, this alternation as well as the loading and unloading of the guideway girders excite vibrations of the ground. In order to calculate the time behavior of the vibrational emissions, a simulation of the transfer of a Transrapid vehicle over several guideway girders is proposed. The equations of motion for the vehicle and the girders are calculated separately by the MBS software NEWEUL and assembled and numerically integrated in MATLAB/SIMULINK. The control law for the magnet forces is simplified by the characteristics of linear spring-damper elements. The controlled magnet forces travel along the guideway continuously and include the dynamic component due to the alternating fluxes and the geometry of the poles and stator. Results of a complete vehicle moving along a guideway consisting of several girders can be obtained within a few minutes of computation time. Therefore, the mechanism of excitations can be analyzed by numerical time integration in the full state space. The results are validated by measurements of the forces in the joints of the guideway girders. The vibrational emission along the Transrapid guideway differs from the vibrations of contact-afflicted vehicles as no impacts and fewer stochastic effects occur.

Keywords Magnetic levitated vehicle · Transrapid · Vibration emission · Discontinuous right-hand side

N. Hägele (✉)
Institute of Engineering and Computational Mechanics, University of Stuttgart, Pfaffenwaldring 9, 70550 Stuttgart, Germany
e-mail: Nora.Haegele@gmx.de

F. Dignath
Basic Technologies, ThyssenKrupp Transrapid, Moosacher Str. 58, 80809 München, Germany
e-mail: Florian.Dignath@ThyssenKrupp.com

1 Introduction

The Maglev vehicle Transrapid as described in [14] and Miller [10] is levitated by magnetic forces which pull the vehicle's levitation frames toward the guideway from below. Therefore, the guideway usually consists of some beam-type elements with a T- or I-shaped cross section. They are often designed as individual concrete girders placed next to each other. The magnets are distributed equally along the vehicle and possess poles with alternating fluxes which are part of the synchronous long stator linear motor. An overview of the design of magnets and guideway is given in [15] and a detailed comparison between the system properties of the Transrapid and the system properties of conventional high-speed trains can be found in [16].

During the transit of a Transrapid vehicle, vibrational forces are transmitted into the ground with various, but well-defined frequencies. As similar vibrations occur with any transportation system or heavy machinery, norms have been defined for the measurement [1] and the evaluation of the resulting immissions into houses, e.g. [2]. The vibrations from a passing Maglev train are excited firstly by the loading and unloading of the separate girders and, secondly, by the alternating fluxes of the poles. Furthermore, excitations with multiples of the pole frequency and pole wavelength occur with smaller amplitudes due to the geometric shape of the magnetic field. All frequencies are proportional to the velocity of the passing vehicle because the wavelengths are given by constant relations from the geometry. Furthermore, stochastic excitations exist, but their amplitudes are small compared to the deterministic excitations as soon as the vehicle takes up speed. The forces of the guiding magnets are small compared to the forces from the levitation magnets and possess no alternating fluxes.

In order to calculate the time behavior of the vibrational emissions depending on the velocity and the parameters of the vehicle and guideway, a simulation of the transit of a Transrapid vehicle over several guideway girders can be applied. Such simulations have been described by various authors with respect to the control problem [4, 7, 12] or with a focus on the guideway reaction to the moving loads [9]. However, the magnet forces are usually modeled as either discrete or smooth continuous forces, neglecting the effects of the alternating poles and the detailed shape of the magnetic field since they are of low significance for control purposes and the global reaction of the guideway. On the other hand, detailed computations with complex finite element models of the guideway and the geometric shape of the magnet poles have been reported [11] in order to describe the vibrational load. Due to the high computation times needed for these guideway models, the dynamic motion of the vehicle is neglected and a constant air-gap between magnets and guideway is assumed in these models.

The work presented here is trying to close the gap between these two different modeling approaches. Therefore, the model is built in a similar way to those used for the computation of the control—including the dynamics of the vehicle and the guideway—but augmented by a detailed modeling of the magnet forces. The control system for the unstable electromagnets is replaced by linear spring-damper elements. With this model, the mechanism of vibrational excitation can be analyzed and measures for the reduction of the resulting emissions can be evaluated. It is particularly useful for the analysis of elastic supports of the guideway girders which are currently being considered in the planning process for a Transrapid track in order to damp the vibrations in sensitive building areas. This paper is based on the diploma thesis [5].

2 Model

Since the vibrational forces are excited mainly by the levitation magnets, the simulation model represents the vertical dynamics of the Transrapid vehicle only. In the following, the design of the levitation and guidance system is described before deriving a two-dimensional vertical model.

This two-dimensional model consists of separate Multibody Systems (MBS) for the vehicle and each guideway girder, allowing a transfer of the vehicle from one girder onto subsequent girders. The mathematical representations of the MBS submodels for vehicle and girders are derived in Sect. 3 and coupled in the simulation model as described in Sect. 4.

2.1 Levitation and guidance system

The magnets are distributed equally along the length of the Transrapid vehicle and follow the guideway position very strictly at the given air-gap distance of about 10 mm. The 16 levitation magnets of each vehicle section (coach) are controlled individually establishing the nearly constant air-gap over the whole length of the vehicle. They are connected by elastic joints leading to chain-like kinematics which allows the magnets to adapt to the guideway layout, such as in curves. An undercarriage distributes the mass forces from the rigid car body equally onto the magnets, while at the same time allowing a flexible motion between each magnet and the car body.

2.1.1 Magnetic undercarriage

As can be seen in Figs. 1 and 2, the undercarriage consists of four levitation chassis per vehicle section. The levitation and guidance magnets are connected to these chassis by elastomer springs in the vertical (z) and longitudinal (x) direction (primary springs) and control arms (not shown) in the transversal direction (y). As every other magnet is mounted between two levitation chassis, a flexible chain of chassis and magnets is achieved. The levitation chassis themselves are connected to the vehicle body via control arms in the x direction and a pendulum design including soft air springs in the y–z-plane (secondary suspension). Overall, there are 16 air springs per vehicle section resulting in a rigid body frequency below 1 Hz, thus decoupling the quick motion of the magnets from the vehicle body. The roll of the car body is prevented by elastomer elements between the left and right air spring rockers as shown in Fig. 1.

2.1.2 Levitation magnets

The force of each levitation magnet is controlled such that it corresponds to the loads from the vehicle onto the magnets while the magnets' position follows the guideway at a given distance (about 10 mm air-gap). The nominal force is given at all times by the mass of the vehicle and its dynamic motion because the corner frequency of the controller is higher than the natural frequencies of the vehicle's components. The force is generated by alternating DC-fluxes ϕ through 12 discrete poles (10 main poles and 2 end poles) which are distributed over the magnet length as shown in Fig. 3. The alternating fluxes are used by the linear motor which consists of three windings placed within the stator slots, also shown in Fig. 3.

The geometry of the poles is detuned with respect to the slots in order to achieve a smooth force distribution. However, some irregularities in the force and especially in its distribution over the magnet length remain and act as a vibrational excitation.

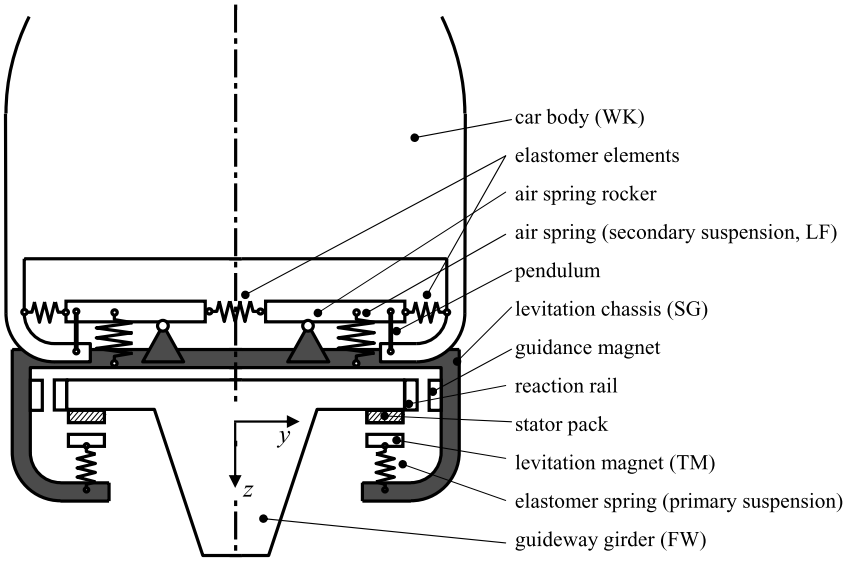

Fig. 1 Cross section through the vehicle

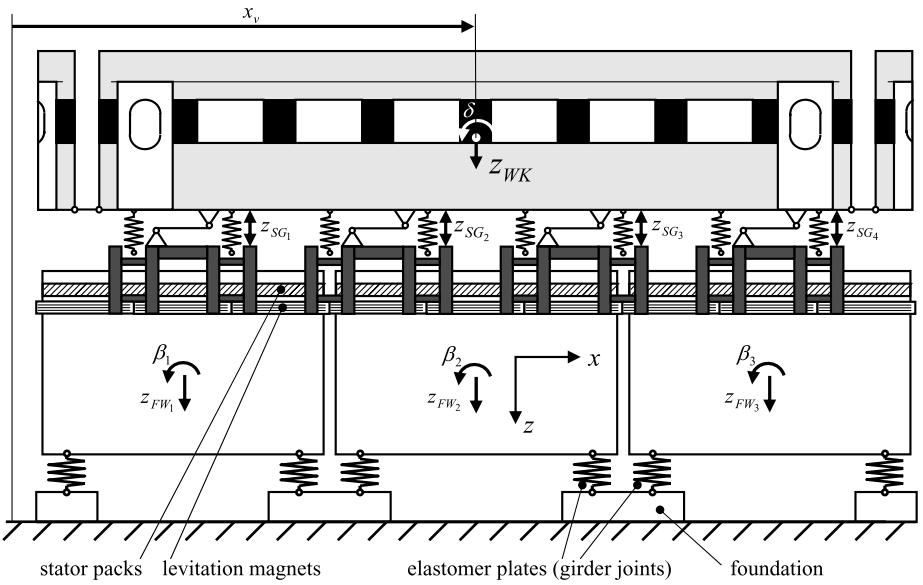

Fig. 2 Side view of the vehicle

2.2 Multibody systems

Since vehicle and guideway are symmetric with respect to the x–z plane, as shown in Fig. 1, a two-dimensional model may be used in order to analyze the vibrational excitation of the guideway during the transfer of the vehicle. By this simplification, the roll and yaw mo-

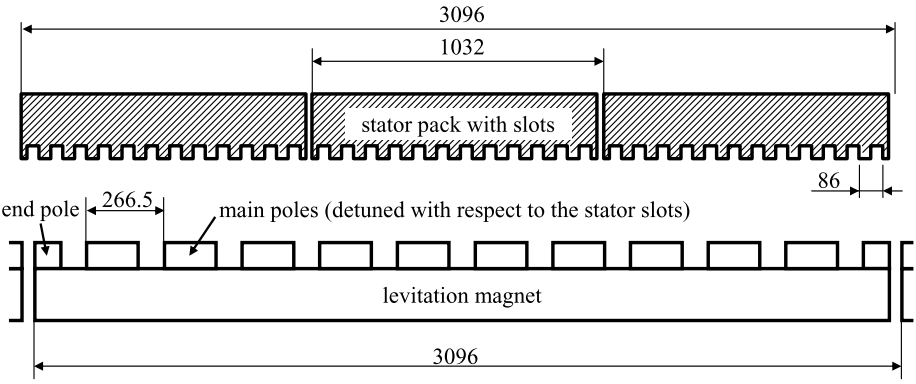

Fig. 3 Geometry of the magnet poles and the stator as given in [3], measures in mm

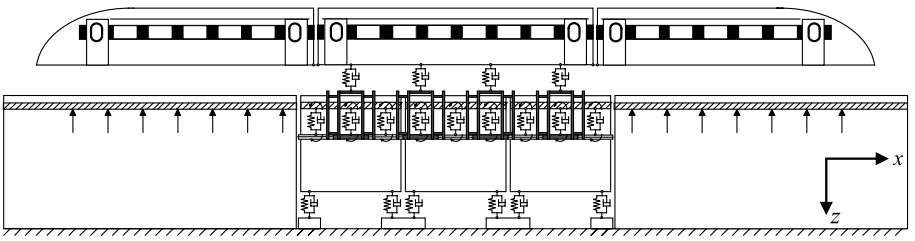

Fig. 4 Multibody system of the complete vehicle and guideway

tions of the vehicle are neglected, which are considered to have only a small influence on the vibrations of the guideway as the corresponding natural frequencies are small and well damped. A further reduction of the dimension of the problem is achieved by considering a transit of the vehicle with constant longitudinal velocity.

By this reduction and by using a rigid multibody system, the number of degrees of freedom is reduced to six for each vehicle section and two for each guideway girder. The model may be augmented in further projects by the more detailed consideration of dynamic properties of the vehicle's undercarriage or the guideway girders, but the presented simplification proved sufficiently detailed for the scope of this work.

In Fig. 4, the two-dimensional model used is shown where all masses and coupling elements represent the added properties of the left and the right vehicle part. In order to allow a transfer of the vehicle from one guideway girder onto the next, a modular approach is applied using several submodels,

– one submodel for each vehicle section,
– one submodel for each guideway girder,
– half-infinite guideway parts at each end as boundary and initial conditions.

These submodels are coupled by the computation of the magnet force.

2.2.1 Model of the vehicle

The Transrapid vehicle considered consists of three sections with a mass of max. 65 t, one middle section, and two end sections. Only the middle section is modeled in detail while the

bow sections are regarded by the nominal loads of the levitation magnets on the guideway. The model of the middle section consists of one rigid body for the car body, four rigid bodies for the levitation chassis and nine rigid bodies for the levitation magnets.

In reality, these magnets are connected to the levitation chassis by primary springs on each side of the vehicle as shown in Fig. 2. However, as the stiffness of the primary springs is high compared to the secondary suspension, its elasticity may be neglected. Therefore, the levitation magnets within the levitation chassis are connected rigidly to them. The levitation magnets in between two levitation chassis are connected by joints to the chassis so that their vertical position is always in the center between the vertical position of the neighboring magnets. As the outermost levitation magnets of the middle section are also acting on the end sections, nine levitation magnets need to be included in the submodel although the length of one section corresponds only to eight magnets.

The definitions of the generalized coordinates

$$\boldsymbol{y}_{FZ}(t) = \begin{bmatrix} z_{SG_1} & z_{SG_2} & z_{SG_3} & z_{SG_4} & z_{WK} & \delta \end{bmatrix}^T \tag{1}$$

and the auxiliary variable $x_v(t)$ are shown in Fig. 2. The auxiliary variable describes the given motion in the longitudinal x-direction.

The four air springs of each levitation chassis, transferring only forces in vertical direction, are modeled by one spring-damper combination neglecting hereby the possible rotation of the levitation chassis versus the car body. The influence of the rotation of the levitation chassis on the vertical dynamics of the systems may be investigated in further studies, but is supposed to be small for the stiff guideways which are generally used. The lever of the air spring rockers seen in Fig. 1 is considered in the force law of the air spring.

2.2.2 *Model of the guideway*

As shown in Fig. 4, each foundation supports two girders on elastomer plates. Therefore, at least three guideway girder models are necessary in order to calculate the loads on the foundations and the motion of the central girder correctly. Furthermore, fixed half-infinite guideway parts are used as boundary conditions for the run-on and run-off of the vehicle.

The guideway considered in this paper consists of separately supported girders with a length of 9.3 m and a mass of about 35 t. They are supported by four joints (one at each corner) that are designed as elastomer plates, presenting a small elasticity between the girder and the foundations. The elastomer plates are compressed approximately 40 µm when fully loaded by the vehicle and are considered by a spring damper combination. The first bending mode of one girder possesses a natural frequency of about 30 Hz. However, as this structural elasticity is not considered, each girder possesses only two degrees of freedom

$$\boldsymbol{y}_{FW}(t) = \begin{bmatrix} z_{FW} & \beta \end{bmatrix}^T . \tag{2}$$

2.2.3 *Coupling of the submodels*

In order to connect the subsystems, a reference plane is introduced as shown in Fig. 5. The distances of the magnets from this reference plane as well as the distances of the corresponding stator packs from this plane are calculated in each subsystem and forwarded to the computation of the magnet force. The magnet forces are then computed based on this information and returned to the vehicle models and, in inverted form, to the subsystems of the corresponding guideway girders.

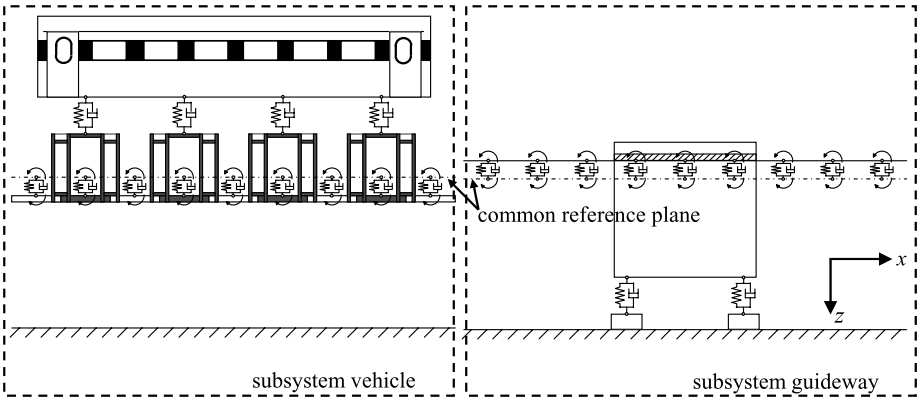

Fig. 5 Separated modeling of train section and guideway girder

The forces and torques acting on the ground from the foundation can be calculated directly from the spring and damper forces of the elastomer plates of the girders. The forces result from the summation of the respective forces on the foundations, while for the torque the corresponding lever arms are considered additionally.

2.2.4 Model of the magnet force

As described in Sect. 2.1.2, the geometry of the magnet poles leads to a vibrational excitation of the guideway girders. Compared to these excitations, the effects of the controller onto the vibrations can be neglected for the investigations presented in this paper. However, the controller produces the nominal force of the magnets corresponding to the dynamic motion of the car body. Therefore, the complex control law is replaced by a linear stiffness and velocity proportional damping (corresponding to a linear spring-damper combination, shown in Figs. 4 and 5). The parameters of the spring-damper elements, used in the simulation, are chosen to $c = 0.14$ kN/mm and $d = 25.98$ Ns/mm; see [5].

For this purpose, the force distribution $q_{\mathrm{mag}}(x)$ is integrated over the length of one magnet L_{TM} leading to a force/torque pair consisting of the net-force $F_{TM}(x_v) = \int_{-L_{TM}/2}^{+L_{TM}/2} q_{\mathrm{mag}}(x, x_v)\,dx$ and the net-torque $M_{TM}(x_v) = \int_{-L_{TM}/2}^{+L_{TM}/2} q_{\mathrm{mag}}(x, x_v)\,x\,dx$ in the center of the magnet. Because of the geometry of poles and stator described above, the force/torque pair $(F, M)_{TM}$ is dependent on the longitudinal position of the vehicle x_v with respect to the guideway

$$(F, M)_{TM}(t) = (\bar{F}, \bar{M})_{TM}\big(\boldsymbol{y}_{FZ}(t), \boldsymbol{y}_{FW}(t)\big) + \Delta(F, M)_{TM}\big(x_v(t)\big). \tag{3}$$

Since the relative force distribution is nearly independent from the overall flux, $\Delta F_{TM}(x_v)$ and $\Delta M_{TM}(x_v)$ can be computed beforehand as percentages of the average nominal values $(\bar{F}, \bar{M})_{TM}$. This percentage value is then multiplied with the force computed in the simulation $(\bar{F}, \bar{M})_{TM}(\boldsymbol{y}_{FZ}(t), \boldsymbol{y}_{FW}(t))$ and presents an external excitation to the system. In the following, the magnet forces and torques of all three vehicle sections (with 23 magnets in total) are assembled in the vectors $\boldsymbol{F}_{TM}$ and $\boldsymbol{M}_{TM}$

$$\begin{aligned} \boldsymbol{F}_{TM}(t) &= [F_{TM1} \quad F_{TM2} \quad \ldots \quad F_{TM23}]^T, \\ \boldsymbol{M}_{TM}(t) &= [M_{TM1} \quad M_{TM2} \quad \ldots \quad M_{TM23}]^T. \end{aligned} \tag{4}$$

3 Equations of motion

The equations of motion for each submodel described in the previous chapter are derived by the Newton–Euler method, implemented in the multibody software package NEWEUL [6].

3.1 Kinematics

In order to set up the equations of motion with the minimal number of coordinates, the positions $\boldsymbol{r}_i$ and velocities $\boldsymbol{v}_i$ of each body i are expressed in terms of the generalized coordinates $\boldsymbol{y}$, i.e., $\boldsymbol{y}_{FZ}$ or $\boldsymbol{y}_{FW}$, respectively. As described in Sect. 2.2, the number of degrees of freedom was reduced by restricting the analysis to a transit of the vehicle with a prescribed velocity. Therefore, the longitudinal motion of all vehicle bodies is described by a time-dependent substitution variable $x_v(t)$ instead of generalized coordinates. The positions $\boldsymbol{r}_i$ of the vehicle bodies depend on this variable which needs to be considered in the time differentiation of the position vectors. The corresponding terms $\partial r/\partial x_v$ are sorted into the vector of local velocities $\bar{\boldsymbol{v}}_i$. As the dependency of $\boldsymbol{r}_i(x_v)$ is linear in the considered model, the local velocities $\boldsymbol{v}_i$ depend on $\dot{x}_v$ and the generalized coordinates only,

$$\boldsymbol{v}_i = \frac{\partial \boldsymbol{r}_i}{\partial \boldsymbol{y}_{FZ}} \cdot \dot{\boldsymbol{y}}_{FZ}(t) + \frac{\partial \boldsymbol{r}_i}{\partial x_v} \dot{x}_v(t) = \boldsymbol{J}_{Ti}(\boldsymbol{y}_{FZ}) \cdot \dot{\boldsymbol{y}}_{FZ}(t) + \bar{\boldsymbol{v}}_i(\boldsymbol{y}_{FZ}, \dot{x}_v). \tag{5}$$

The motion of the guideway girders is only dependent on the generalized coordinates $\boldsymbol{y}_{FW}$ so that the local velocity $\bar{\boldsymbol{v}}_i$ is equal to zero for the guideway.

A further differentiation yields the accelerations, which can be divided into the local accelerations $\bar{\boldsymbol{a}}_i$ and an acceleration part depending on the generalized coordinates only. For the vehicle considered, the local accelerations depend on the second derivative of the auxiliary variable and the generalized coordinates. For the transit with constant velocity, the second derivative $\ddot{x}_v$ amounts to zero

$$\boldsymbol{a}_i = \boldsymbol{J}_{Ti}(\boldsymbol{y}_{FZ}) \cdot \ddot{\boldsymbol{y}}_{FZ}(t) + \bar{\boldsymbol{a}}_i(\boldsymbol{y}_{FZ}, \dot{\boldsymbol{y}}_{FZ}, \ddot{x}_v). \tag{6}$$

The rotations are not directly dependent on x_v and can be formulated as

$$\boldsymbol{\omega}_i = \boldsymbol{J}_{Ri} \cdot \dot{\boldsymbol{y}}_{FZ}(t) + \bar{\boldsymbol{\omega}}(=0), \tag{7}$$

$$\boldsymbol{\alpha}_i = \boldsymbol{J}_{Ri} \cdot \ddot{\boldsymbol{y}}_{FZ}(t) + \bar{\boldsymbol{\alpha}}(=0), \tag{8}$$

with constant Jacobian matrices $\boldsymbol{J}_{Ri}$. The equations for the guideway can be set up accordingly using the generalized coordinates $\boldsymbol{y}_{FW}$. They are not dependent on the auxiliary variable.

3.2 Kinetics

The accelerations of the systems according to (6) and (8) are effected by the forces and torques acting on the different bodies. The influence of these forces and torques on free bodies is described by the equations of Newton and Euler.

Using the Jacobian matrices $\boldsymbol{J}_{Ti}$ and $\boldsymbol{J}_{Ri}$ from (6) and (8), these can be written in matrix notation as

$$\overline{\overline{\boldsymbol{M}}} \cdot \overline{\boldsymbol{J}} \cdot \ddot{\boldsymbol{y}}(t) + \overline{\boldsymbol{k}}(t) = \overline{\boldsymbol{q}}^e + \overline{\boldsymbol{q}}^r, \tag{9}$$

where the block diagonal matrix $\overline{\overline{\boldsymbol{M}}} = \mathrm{diag}\{m_1\boldsymbol{E}\ m_2\boldsymbol{E}\ \ldots\ m_p\boldsymbol{E}\ \boldsymbol{I}_1\ \ldots\ \boldsymbol{I}_p\}$ contains the masses and moments of inertia of all p bodies, $\overline{\boldsymbol{J}} = [\boldsymbol{J}_{T1}^T\ \boldsymbol{J}_{T2}^T\ \ldots\ \boldsymbol{J}_{Tp}^T\ \boldsymbol{J}_{R1}^T\ \ldots\ \boldsymbol{J}_{Rp}^T]^T$ represents the global Jacobian matrix, and

$$\overline{\boldsymbol{k}} = \left[m_1\bar{\boldsymbol{a}}_1 \quad m_2\bar{\boldsymbol{a}}_2 \quad \ldots \quad m_p\bar{\boldsymbol{a}}_p \quad \boldsymbol{I}_1\cdot\bar{\boldsymbol{\alpha}}_1 + \widetilde{\boldsymbol{\omega}}_1\cdot\boldsymbol{I}_1\cdot\boldsymbol{\omega}_1 \quad \ldots \quad \boldsymbol{I}_p\cdot\bar{\boldsymbol{\alpha}}_p + \widetilde{\boldsymbol{\omega}}_p\cdot\boldsymbol{I}_p\cdot\boldsymbol{\omega}_p\right]^T \tag{10}$$

contains the generalized Coriolis, centrifugal and gyroscopic forces, derived from the local accelerations in (6) and (8). On the right-hand side of (9) the internal and external forces $\boldsymbol{f}_i$ and torques $\boldsymbol{l}_i$ acting on each body are separated into the vector $\overline{\boldsymbol{q}}^e$ of the generalized applied forces and the vector $\overline{\boldsymbol{q}}^r$ of the generalized reaction forces,

$$\overline{\boldsymbol{q}}^{e/r} = \left[\boldsymbol{f}_1^{e/r} \quad \boldsymbol{f}_2^{e/r} \quad \ldots \quad \boldsymbol{f}_p^{e/r} \quad \boldsymbol{l}_1^{e/r} \quad \ldots \quad \boldsymbol{l}_p^{e/r}\right]. \tag{11}$$

For the vehicle, the local accelerations and, therefore, the vector $\overline{\boldsymbol{k}}$ in (10) is dependent on the second derivative of the auxiliary variable. Furthermore, the auxiliary variable needs to be considered when calculating the vector of applied forces $\overline{\boldsymbol{q}}^e$ as the position of the forces $\boldsymbol{F}_{TM}$ from (4) depends on $x_v(t)$ thereby creating a torque on the guideway. Therefore, terms depending on x_v and $\dot{x}_v$ can exist in the vectors $\boldsymbol{f}^e$ and $\boldsymbol{l}^e$ in (11) for the vehicle and for the guideway. The Newton–Euler equations for the vehicle read as

$$\begin{aligned}\overline{\overline{\boldsymbol{M}}}_{FZ}(\boldsymbol{y}_{FZ})\cdot\overline{\boldsymbol{J}}_{FZ}(\boldsymbol{y}_{FZ})\cdot\ddot{\boldsymbol{y}}_{FZ}(t) + \overline{\boldsymbol{k}}_{FZ}(\boldsymbol{y}_{FZ},\dot{\boldsymbol{y}}_{FZ},\ddot{x}_v)\\ = \overline{\boldsymbol{q}}^e_{FZ}(\boldsymbol{y}_{FZ},\dot{\boldsymbol{y}}_{FZ},x_v,\dot{x}_v) + \overline{\boldsymbol{q}}^r_{FZ}(t).\end{aligned} \tag{12}$$

For the guideway and/or for a transit with constant velocity, only the right hand side of the Newton–Euler equations depends on the auxiliary variable.

3.3 Equations of motion

The reaction forces $\overline{\boldsymbol{q}}^r$ in (9) and (12) do not directly influence the motion of the system along the generalized coordinates $\boldsymbol{y}$. The Newton–Euler equations can, therefore, be reduced into a system of minimal coordinates. For this, the multibody software NEWEUL applies d'Alemberts principle, eliminating the reaction forces by premultiplication of the Newton–Euler equations with the transposed global Jacobian matrix $\overline{\boldsymbol{J}}^T$. The equations of motion for the vehicle then read as

$$\begin{aligned}\boldsymbol{M}_{FZ}(\boldsymbol{y}_{FZ})\cdot\ddot{\boldsymbol{y}}_{FZ}(t) + \boldsymbol{k}_{FZ}(\boldsymbol{y}_{FZ},\dot{\boldsymbol{y}}_{FZ},\ddot{x}_v)\\ = \boldsymbol{q}_{FZ}(\boldsymbol{y}_{FZ},\dot{\boldsymbol{y}}_{FZ},x_v,\dot{x}_v),\end{aligned} \tag{13}$$

where $\boldsymbol{M}_{FZ} = \overline{\boldsymbol{J}}^T_{FZ}\cdot\overline{\overline{\boldsymbol{M}}}_{FZ}\cdot\overline{\boldsymbol{J}}_{FZ}$ is the symmetric, positive definite mass matrix, $\boldsymbol{k}_{FZ} = \overline{\boldsymbol{J}}^T_{FZ}\cdot\overline{\boldsymbol{k}}_{FZ}$ represents the vector of generalized Coriolis, gyroscopic and centrifugal forces and $\boldsymbol{q}_{FZ} = \overline{\boldsymbol{J}}^T_{FZ}\cdot\overline{\boldsymbol{q}}^e_{FZ}$ is the vector of the generalized applied forces containing, amongst others, the external magnet forces and torques from (4). For the guideway and for a transit with constant velocity, only the right-hand side of the equations of motion depends on the auxiliary variable $x_v(t)$. A more detailed description can also be found in the text book [17].

All generalized coordinates describe small deviations about the equilibrium position. A linearization about this equilibrium $\boldsymbol{y}_0$ with $\boldsymbol{y}(t) = \boldsymbol{y}_0 + \boldsymbol{\eta}(t)$, $\dot{\boldsymbol{y}}(t) = \dot{\boldsymbol{\eta}}(t)$ and $\ddot{\boldsymbol{y}}(t) = \ddot{\boldsymbol{\eta}}(t)$

and the consideration of a transit with constant velocity $\dot{x}_v = \text{const.}$ lead to equations of the form

$$\boldsymbol{M}_0 \cdot \ddot{\boldsymbol{\eta}}(t) + \boldsymbol{P} \cdot \dot{\boldsymbol{\eta}}(t) + \boldsymbol{Q} \cdot \boldsymbol{\eta}(t) = \boldsymbol{h}(\boldsymbol{y}, \dot{\boldsymbol{y}}, x_v, \dot{x}_v) \tag{14}$$

for the vehicle as well as for the guideway with constant matrices on the left-hand side.

4 Simulation

The equations of motion of the subsystems for each vehicle section and each guideway girder are coupled on the mathematical level and solved by numerical time integration using the program MATLAB/SIMULINK [18]. A detailed consideration of the distribution of the magnet forces achieves a continuous right-hand side of the differential equations.

4.1 State equations of the subsystems

The equations of motion set up in the linear form (14) using NEWEUL are transferred to MATLAB for further calculations. The differential equations are solved by numerical time integration using standard algorithms. They are thus transformed into the standard form of first order state equations defining $\boldsymbol{x} = [\,\boldsymbol{y}\;\dot{\boldsymbol{y}}\,]^T$ where $\boldsymbol{y}$ is $\boldsymbol{y}_{FZ}$ or $\boldsymbol{y}_{FW}$, respectively,

$$\dot{\boldsymbol{x}}(t) = \boldsymbol{A}(t) \cdot \boldsymbol{x}(t) + \boldsymbol{B}(t) \cdot \boldsymbol{u}(t), \qquad \boldsymbol{x}(t_0) = \boldsymbol{x}_0, \tag{15}$$

$$\boldsymbol{y}_{\text{out}}(t) = \boldsymbol{C}(t) \cdot \boldsymbol{x}(t) + \boldsymbol{D}(t) \cdot \boldsymbol{u}(t), \tag{16}$$

where $\boldsymbol{A}(t)$ is called the system matrix, $\boldsymbol{B}(t)$ the input matrix, $\boldsymbol{C}(t)$ the output matrix and $\boldsymbol{D}(t)$ the straight-way matrix. For the simplified control law for the magnets used in this paper, matrices $\boldsymbol{C}$ and $\boldsymbol{D}$ are defined such that $\boldsymbol{y}_{\text{out}} = \boldsymbol{x}$. The product $\boldsymbol{B}(t) \cdot \boldsymbol{u}(t)$ contains the vector of excitations $\boldsymbol{h}(t)$ from equations in the form of (14). Therefore, $\boldsymbol{h}(t)$ is split into a distribution matrix and a vector of independent inputs $\boldsymbol{h} = \boldsymbol{Q}_e \cdot \boldsymbol{u}$ with

$$\boldsymbol{u}_{FZ}(t) = \begin{bmatrix} \boldsymbol{F}_{TM} \\ \boldsymbol{M}_{TM} \\ \boldsymbol{F}_{LF} \\ m_{WK}\, g \\ \boldsymbol{m}_{SG/TM}\, g \end{bmatrix}, \qquad \boldsymbol{u}_{FW}(t) = \begin{bmatrix} \boldsymbol{F}_{TM} \\ x_v\, \boldsymbol{F}_{TM} \\ \boldsymbol{M}_{TM} \\ \boldsymbol{F}_{FW} \\ m_{FW}\, g \end{bmatrix}. \tag{17}$$

Here, $\boldsymbol{F}_{TM}(\boldsymbol{y}_{FZ}, \dot{\boldsymbol{y}}_{FZ}, \boldsymbol{y}_{FW}, \dot{\boldsymbol{y}}_{FW}, x_v, \dot{x}_v)$ and $\boldsymbol{M}_{TM}(\boldsymbol{y}_{FZ}, \ldots, \dot{x}_v)$ represent the magnet forces and torques. The movement of the magnet forces along the guideway changes their lever arms with respect to the guideway, thereby creating the additional torque $x_v(t)\, \boldsymbol{F}_{TM}$ in the vector $\boldsymbol{u}_{FW}$. The air-spring forces $\boldsymbol{F}_{LF}(\boldsymbol{y}_{FZ}, \dot{\boldsymbol{y}}_{FZ})$ and the forces of the guideway bearings $\boldsymbol{F}_{FW}(\boldsymbol{y}_{FW}, \dot{\boldsymbol{y}}_{FW})$ are extracted from the matrices $\boldsymbol{P}$ and $\boldsymbol{Q}$ in (14) so they are available as output quantities in the SIMULINK model and a nonlinear computation of them may be introduced in a subsequent work. Furthermore, the weight of the passenger cabin and the guideway $m_{WK}\, g$ and $m_{FW}\, g$ as well as the weight of the levitation chassis and levitation magnets $\boldsymbol{m}_{SG/TM}\, g$ are introduced as inputs in order to consider the constant forces in the state equations.

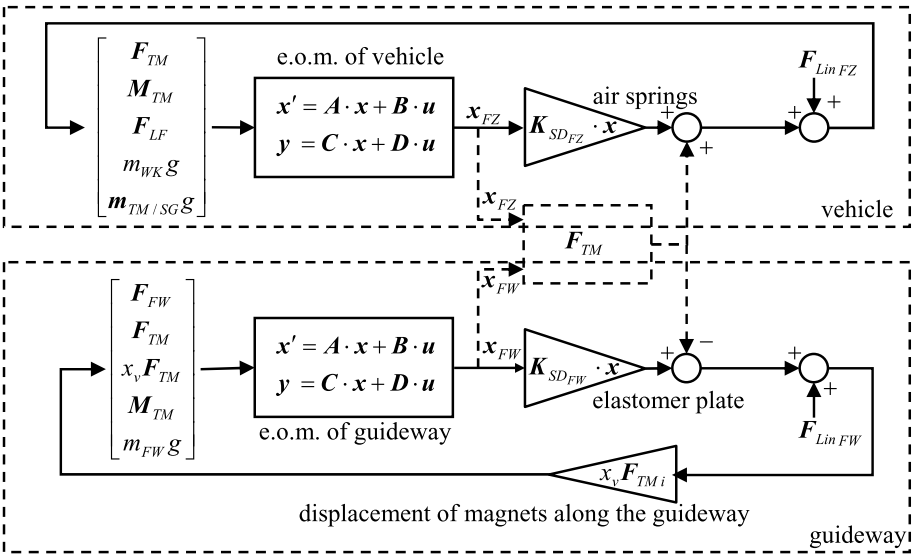

Fig. 6 Connection of the different part systems in SIMULINK

4.2 Coupling of vehicle and guideway

The numerical integration of the system is performed with the program SIMULINK, where the coupling of both subsystems is described by a graphical interface. The subsystems and calculation procedures are described by block elements which are connected by several inputs and outputs. The block elements contain the equations and matrices described in the previous section. As the coupling of the system elements takes place before the numerical integration, it is a coupling on the mathematical level.

Within those system elements, the state space equations created in Matlab are given as shown in Fig. 6. The force elements of the air-springs of the vehicle and the elastomer plates of the girder are given as stiffness and damping matrices which are set up beforehand in Matlab. The nominal forces in the linearization point are added as additional constants. The system elements for the guideway girder are contained three times in the overall model in order to describe the three girders as shown in Fig. 4.

The subsystems of a vehicle section and each guideway girder are coupled by the computation of the magnet forces as shown in Fig. 6. The levitation magnet force is dependent on the generalized coordinates of both subsystems and is described in detail in the following subsection.

4.3 Computation of the magnet force

As described in Sect. 2.2.4, the controlled magnet forces are modeled as displacement and velocity proportional forces F_{TM} and M_{TM} representing the integral of the force distribution over one magnet. For the control law with parameters c_{TM} and d_{TM}, the distance Δr_i and relative velocity Δv_i between each magnet i and the stator is computed from the generalized coordinates $\boldsymbol{x}_{FZ}$ of the vehicle and $\boldsymbol{x}_{FW}$ of the guideway, as shown in Fig. 7. The relation between the generalized coordinates and the relative distance and velocity is calculated by a

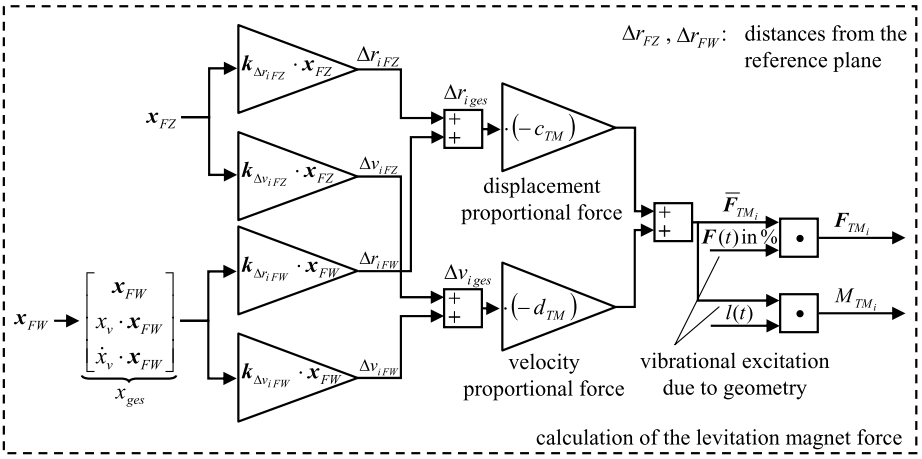

Fig. 7 Computation of the magnet forces in SIMULINK

linear approximation of the equations in the NEWEUL output files for the observer quantities. Switches are used in SIMULINK to assign the corresponding guideway to each magnet i dependent on the vehicle's position x_v.

After the nominal force has been calculated, the vibrational excitation due to the geometry of the poles and stator as described in Sect. 2.2.4 is considered by a factor for F_{TM_i}, while the torque M_{TM_i} is generated using a precomputed lever $l_i(x_v)$, so that $M_{TM_i}(x_v) = l_i(x_v) F_{TM_i}(x_v)$. The influence of this excitation is shown in Fig. 8. In these factors, the run-on and run-off of the magnet to/from one guideway girder are also included. The run-on and run-off lead to a continuous increase or decrease of the force and torque. Therefore, the switches for assigning the corresponding guideway girders to each magnet previously described do not lead to discontinuities in the time behavior but only to nondifferential points in the accelerations. These nondifferential points can be handled by the Runge–Kutta integrator of SIMULINK without special adaptations. However, a more simplified representation of the magnet forces may lead to discontinuities as described in [8] and [13].

4.4 Overall model of three vehicle sections and guideway girders

For the main model, several vehicle sections and guideway girders need to be considered, as described in Sect. 2. For the purpose of this paper, the middle section of a three section vehicle is modeled dynamically as shown in Fig. 6. The bow sections are considered by their nominal magnet forces only. Their motion when traveling over the guideway as well as their influence on the magnet forces are, therefore, not considered. However, the force variation due to the geometry of the magnet poles and the stator as shown in Fig. 8 is included. As the shared levitation magnets between the bow and middle sections are already considered in the dynamic model of the middle section only seven levitation magnets for each bow section remain.

As shown in Fig. 4, three guideway girders are modeled dynamically. Therefore, the corresponding system blocks from Fig. 6 are introduced three times identically but with different input and output quantities. In order to allow a full transfer of the complete vehicle over all three girders, half-infinite guideway parts are additionally added on both sides. These half-infinite parts act as boundary conditions and possess no degrees of freedom. Logical

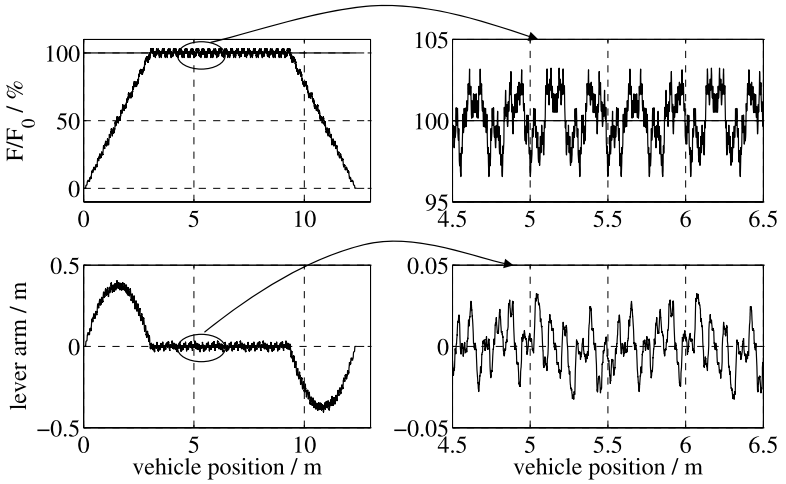

Fig. 8 Factors for force and torque of one magnet traveling over a girder of 9.3 m length, including the vibrational excitation due to the geometry of poles and stator slots

switches define the connection between the three vehicle sections and the guideway parts, while the run-on and run-off contained in the factors shown in Fig. 8 ensure smooth and differentiable trajectories of the state variables.

The purpose of the overall model is to describe the vibrational emission of the forces into the ground. As shown in Fig. 2, each foundation is loaded by the forces from two girders. In order to compute the overall vibrational emission, the forces of the elastomer plates of the girders located on the same foundation are added up to one single force and the corresponding torque.

5 Simulation results—validation and parameter studies

After a validation of the simulation results by a comparison with measurements at the girder joints, the resulting vibrational excitation of the foundations are analyzed. A parameter variation reveals the influence of several mechanical properties of the system on the vibration amplitudes.

5.1 Validation of the model

For the verification of the model, the forces in the elastomer plates of the guideway girder are compared with measurements. The 9.3 m long girders considered are tested on the Transrapid Test Track in Emsland (TVE) in Northern Germany. Using very accurate inductive displacement sensors, the deformations of the elastomer plates were recorded during a transfer of the vehicle with different velocities. From these displacements in the range of 50 μm for the full vehicle weight, the corresponding displacement proportional forces can be derived. These are compared to the forces of the corresponding springs in the simulation model. The displacements are recorded at all four elastomer plates over time. As the simulation model is only two-dimensional, the sum of the inner and outer elastomer plates in the measurements is used for comparison with the simulation results.

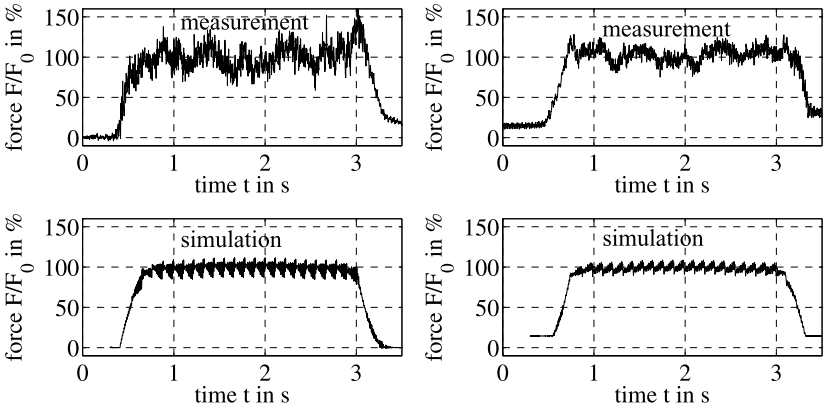

Fig. 9 *Top*: measured data, *bottom*: simulation data. *Left*: Force variation of the incoming joint, *right*: force variation of the outgoing joint. Velocity: $v = 100$ km/h

In Fig. 9, this comparison is shown for the transfer of a three section vehicle at a velocity of 100 km/h. The figure shows that the amplitudes as well as the increase and decrease of the force of the simulation agree reasonably. A comparison of the vibrations caused by the end and middle section in the simulation indicates that the motion of the vehicle does not possess a significant influence on the forces of the foundation joints. The force at the outgoing joint is not exactly zero without the load of the vehicle which shows the existence of a pretension in the springs.

In addition to the trajectory of the simulation, the measurements show a vibration with a very small frequency corresponding to half the length of one vehicle section. This is due to the forces from the guidance magnets. Since the girders on the TVE test track are mounted in a tight curve ($R = 1000$ m), the rigid car body generates clamping forces on the magnetic undercarriage, which adapts to the curve. These forces lead to alternating forces on the guidance magnets at the ends and the center of each section which also influence the corresponding forces of the levitation magnets by the displacement of the levitation chassis. Furthermore, the measured curve shows a slightly longer deflection than the length of the train. This could be explained either by the drift of the measuring instruments, which can be seen at the remaining force after the passing of the vehicle, or by a rotation of the girder foundations due to the unbalanced load of the two girders directly after the vehicle has passed.

For a more detailed comparison of the results, the trajectories are filtered using a small bandwidth filter. As it is known that the strongest vibrational excitation acts with frequencies corresponding to the period lengths of the levitation magnets and the poles, bandwidth filters are applied which extract the corresponding frequencies from the trajectories in Fig. 9. The results are shown in Figs. 10 and 11 at a velocity of 100 km/h. Not regarding some irregularities in the measured data, the vibration amplitudes as well as the time behavior of the simulation and the measurement show good agreement.

5.2 Simulation results

The vibrational emission into the ground arises at each foundation as the sum of the forces of two adjacent girders. In Fig. 12, the resulting force and the corresponding torque acting on the foundation are shown for the transfer with 100 km/h from Fig. 9. The force and the

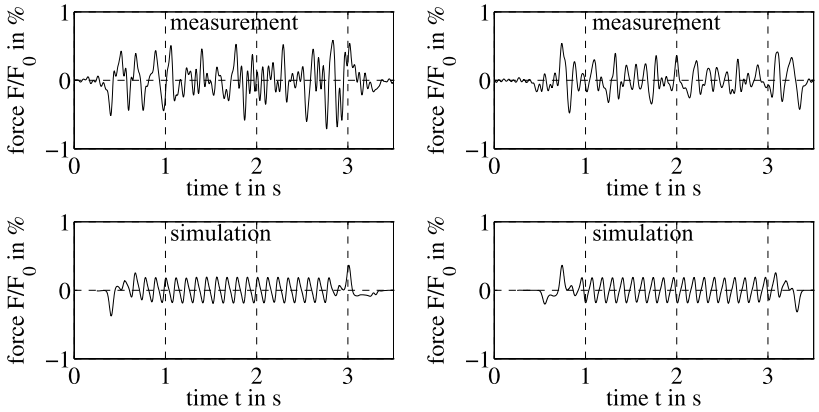

Fig. 10 Data from Fig. 9 filtered around the period length of the levitation magnets at $v = 100$ km/h. *Left*: incoming joint, *right*: outgoing joint

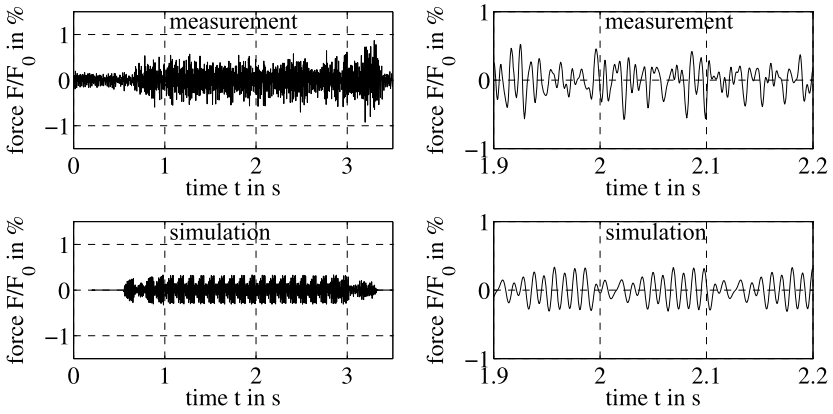

Fig. 11 Data from Fig. 9 filtered around the period length of the magnet poles at $v = 100$ km/h with a more detailed view on the right. *Top*: measured data, *bottom*: simulation data

torque are hereby calculated as shown in Sect. 2.2 using the spring and damper forces of the girder joints as inputs and are normalized by the force F_0 and torque M_0. The force F_0 represents the acting force on the foundation in the equilibrium, while the torque M_0 is defined as the maximum possible torque arising when the train is completely covering one guideway girder.

The influence of the levitation magnet period and the pole period can be seen especially in the torque. Furthermore, the influence of the heavier middle section can be seen by the stronger deflection.

5.3 Frequency analysis of the simulation data

The overall effect of the vibrational load containing various frequencies can be evaluated by a Fourier analysis. Such a frequency analysis of the guideway motion is given in Fig. 13. Next to the excitation frequencies according to the magnet, pole and stator slot periods,

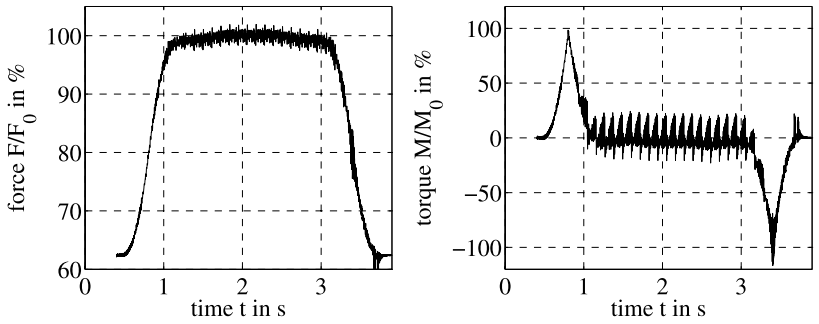

Fig. 12 Percentage force variation in the foundation for a transfer at 100 km/h

vibrations exist at further frequencies which correspond to multiples of the slot period as well as to parts of the magnet period. As all of these excitation frequencies are due to fixed geometric relations, they vary in proportion to the train velocity. In Fig. 13, the results are shown for a transfer of the vehicle at velocities of 80, 100 and 120 km/h.

It can be seen that excitation frequencies near to the translational and rotational eigenfrequency ($f_{e,\mathrm{trans}}$ and $f_{e,\mathrm{rot}}$) of the guideway result in higher vibration amplitudes because of the resonance phenomena. Outside this frequency range the amplitudes are nearly independent of the vehicle velocity. As the structural eigenfrequencies of the real guideway girder are found at lower frequencies (about 20–30 Hz) than the eigenfrequencies of the rigid guideway girder (63 and 100 Hz), further resonances arise in reality which cannot be computed with the simplified rigid simulation model.

5.4 Parameter studies

Finally, the influence of varying or uncertain parameters on the vibrations shall be regarded. For the examination of the influence on the vibrations only one parameter is changed at a time while the others are kept at their initial values. The results of the different simulations show that especially the load of the train section, the inertia of the guideway and the spring and damper values of the elastomer plates of the girder joints have an important influence on the vibrations.

The influence of the spring stiffness of the guideway girders is investigated in combination with the pretension in the springs in order to get the same deflection. A comparison of two different spring stiffnesses reveals that the softer spring leads to slightly larger amplitudes at frequencies corresponding to the pole periods and a steeper increase and decrease of the force in the loading and unloading phase. The variation of the damping coefficient of the elastomer plates of the girder joints influences the amplitudes corresponding to the pole and magnet periods as shown in Fig. 14. It can be deduced that a significant increase of the damping properties for the elastomer joints is a possible means of reducing the vibration of the foundation.

6 Summary

A model is presented for the simulation of the vertical motion of the MAGLEV vehicle Transrapid. This model is used to simulate the transfer of the vehicle over a series of independently supported guideway girders and the resulting vibrations are analyzed.

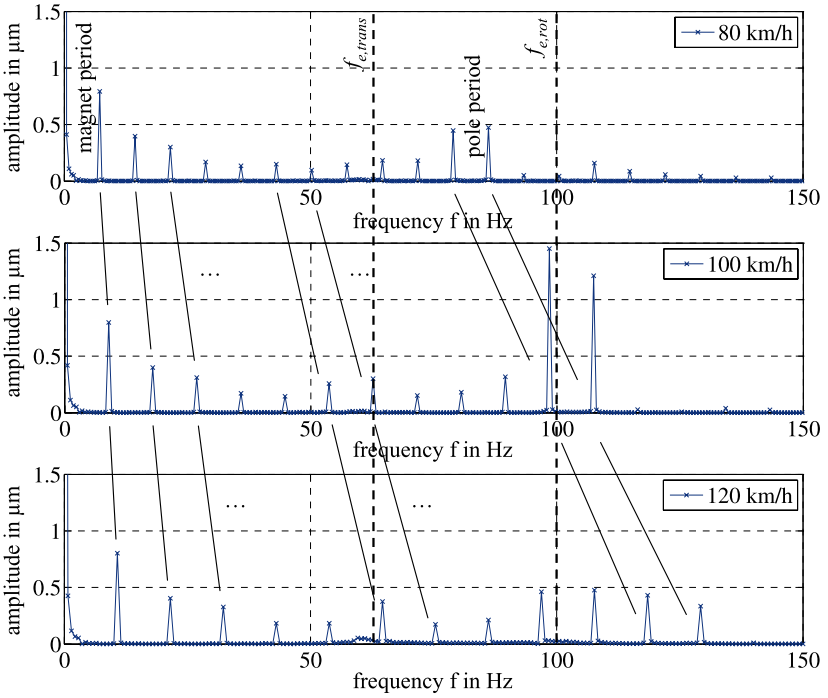

Fig. 13 Frequency analysis of the guideway girder movements at a speed of 80, 100, and 120 km/h

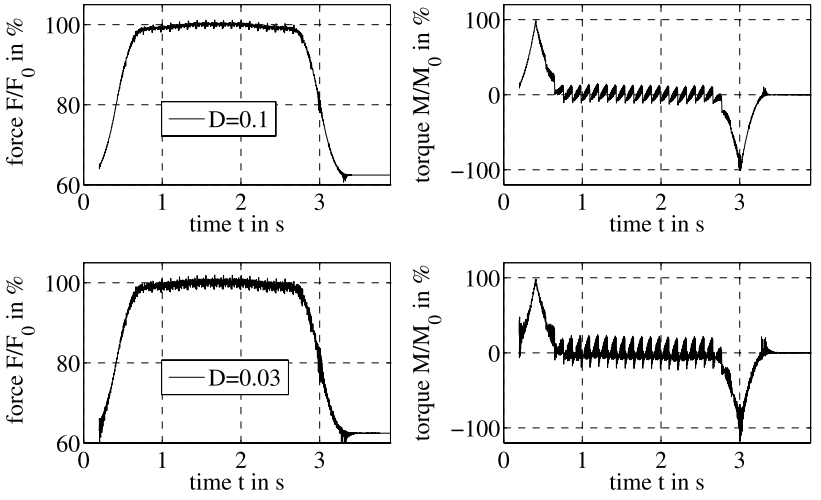

Fig. 14 Force and torque variation in the foundation by varying the damping coefficient of the elastomer joints of the guideway girder

For the modeling, the method of MBS using the software package NEWEUL is applied to the vehicle and to the guideway girders yielding two separate models. The equations of

motion of these models are linked on a mathematical level before running the simulation in SIMULINK. The vehicle consists of three sections. In order to keep the model small, the vehicle travels with constant velocity along the guideway and the front and rear sections are considered by their nominal magnet forces only. Only the middle section is modeled in detail. Rigid links are applied for the connection of the magnets toward the vehicle's levitation chassis. The guideway consists of three dynamically moving girders and fixed half-infinite guideway parts at each end representing the boundary conditions.

Close attention has been paid to the modeling of the forces between the levitation magnets and the guideway. A simple yet detailed solution has been found by assuming displacement and velocity proportional nominal loads for the center of each magnet (thereby the complex control law is replaced by linear spring-damper properties) and a distribution of these loads over the magnet length dependent on the longitudinal position with respect to the guideway. While the nominal load represents the action of the magnet control in a simplified manner, the distribution over the magnet length considers the geometric relations between the 12 poles of each magnet towards the stator possessing 36 slots over the length of one magnet. The geometric relations can be computed offline beforehand depending on the longitudinal position and are introduced as an external excitation in the simulation.

The results show that the model is well suited for an analysis of the vehicle transfer and the resulting vibrations onto the ground. With the parameters of fairly stiff guideway girders considered, the vehicle's motion is small. However, the qualitative effect is shown and the amplitudes depend on the guideway parameters. For soft guideway designs, the consideration of the resulting vehicle motion needs to be included in the vibration analysis.

The guideway motion is characterized by the loading and unloading of the girders with the nominal load of the vehicle. Additionally, vibrations are excited by the force distribution over the magnets, which are transferred into the ground via the guideway joints. The results are analyzed in the frequency domain as well as in the time domain. They show good agreement with measurements—even in the increase and decrease of vibrational amplitudes in the time domain. However, as the girders are modeled as rigid bodies only, the resonance effects near the natural vibrations due to the elastic properties of the girders are not included.

As the models of the vehicle and guideway girders are quite simplified, the presented work can be considered as the starting point for a meticulous theoretical analysis using more and more detailed models. Depending on the particular focus of the investigation, these models could include the natural vibrations of each guideway girder, the magnetic flux at the magnets or the detailed consideration of the control laws. However, even with the simplified model presented, the method proves well suited for analyzing the vehicle and guideway motions simultaneously. This is especially important for investigating the effects of soft guideway parts, which are currently considered for the vibrational isolation near sensitive building areas.

Acknowledgements The authors want to thank Professor P. Eberhard of the Institute of Engineering and Computational Mechanics of the University of Stuttgart, Germany, for his personal supervision and for his kind support of the presented work. Furthermore, we express our sincere thanks to Professor W. Schiehlen for his help in initiating the work and providing important contacts. We acknowledge the contribution of the company "Max Bögl" by kindly and openly providing the parameter values and the measurement results for the guideway girder. We further acknowledge the careful execution of the measurements by W. Nieters of the IABG Lathen and his help in interpreting the results. Furthermore, we thank L. Hawker for the careful language and grammar polishing.

References

1. Deutsches Institut für Normung: Messung von Schwingungsimmissionen. DIN–Norm, DIN 45669 (1995)
2. Deutsches Institut für Normung: Erschütterungen im Bauwesen. DIN–Norm, DIN 4150 (2001)
3. Eisenbahn Bundesamt: Regeln der Technik—Magnetschnellbahn Ausführungsgrundlagen, Gesamtsystem. Published on EBA's website, Doc.-no. 50630 (2006)
4. Gottzein, E.: Das Magnetische Rad als autonome Funktionseinheit modularer Trag- und Führsysteme für Magnetbahnen. VDI–Fortschritt-Berichte, Reihe 8, vol. 68. VDI Verlag, Düsseldorf (1984)
5. Hägele, N.: Vertikaldynamik der Magnetschwebebahn Transrapid unter besonderer Berücksichtigung der Fahrwegdynamik. Diploma Thesis DIPL–112, Institute B of Mechanics, University of Stuttgart (2006)
6. Kreuzer, E., Leister, G.: Programmsystem NEWEUL'90. Institute B of Mechanics, University of Stuttgart, AN-24 (1991)
7. Meisinger, R.: Beträge zur Regelung einer Magnetschwebebahn auf elastischem Fahrweg. Ph.D. thesis, Fachbereich für Maschinenwesen, Technical University of Munich (1977)
8. Meisinger, R.: Optimale Regelung periodischer Systeme mit sprungförmiger Zustandsänderung. Z. Angew. Math. Mech. **57**, T79–T81 (1977)
9. Meisinger, R.: Simulation of a single and double-span guideway under action of moving maglev vehicles with constant force and constant gap. Schriftenreihe der Georg-Simon-Ohm-Fachhochschule Nürnberg (14) (2002)
10. Miller, L.: Transrapid, Innovation für den Hochgeschwindigkeitsverkehr. Bayerischer Monatsspiegel (4), 34–45 (1998)
11. Müller, G., Lutzenberger, S.: Vibrations induced by maglev-trains—a hybrid numerical-analytical-engineering approach. In: Proc. of the 6th German Japanese Bridge Symposium, München (2005)
12. Popp, K.: Beiträge zur Dynamik von Magnetschwebefahrzeugen auf geständerten Fahrwegen. VDI–Fortschritt-Berichte, Reihe 12, vol. 35. VDI Verlag, Düsseldorf (1978)
13. Popp, K., Schiehlen, W.: Dynamics of magnetically levitated vehicles on flexible guideways. In: Pacejka, H. (ed.) The Dynamics of Vehicles on Roads and on Railway Tracks, pp. 479–503. Swets & Zeitlinger B.V., Amsterdam (1976)
14. Raschbichler, H.G.: Entwicklungslinie Magnetschnellbahn Transrapid. In: Rausch, K.F., Rießberger, K., Schaber, H. (eds.) Sonderheft Transrapid. ZEVrail, Glasers Annalen, vol. 127, pp. 10–16. Georg Siemens Verlag, Berlin (2003)
15. Rausch, K.F., Rießberger, K., Schaber, H.: Sonderheft Transrapid. ZEVrail, Glasers Annalen, vol. 127. Georg Siemens Verlag, Berlin (2003)
16. Schach, R., Jehle, P., Naumann, R.: Transrapid und Rad–Schiene–Hochgeschwindigkeitsbahn. Springer, Berlin (2006)
17. Schiehlen, W., Eberhard, P.: Technische Dynamik. Teubner, Wiesbaden (2004)
18. The Mathworks: MATLAB/SIMULINK. Version 7, R14. www.themathworks.com (2005)